



Published in final edited form as:

Oncogene. 2017 January 05; 36(1): 84–96. doi:10.1038/onc.2016.178.

Microphthalmia-Associated Transcription Factor Suppresses Invasion by Reducing Intracellular GTP Pools

Anna Bianchi-Smiraglia^{a,#}, Archis Bagati^{a,#}, Emily E. Fink^a, Sudha Moparthy^a, Joseph A. Wawrzyniak^{a,\$}, Elizabeth K. Marvin^a, Sebastiano Battaglia^b, Peter Jowdy^a, Maria Kolesnikova^a, Colleen E. Foley^a, Albert E. Berman^c, Nadezhda I. Kozlova^c, Brittany C. Lipchick^a, Leslie M. Paul-Rosner^a, Wiam Bshara^d, Jeff Ackroy^e, Donna S. Shewach^e, and Mikhail A. Nikiforov^{a,*}

^aDepartment of Cell Stress Biology, Roswell Park Cancer Institute, Buffalo, New York, 14263

^bDepartment of Pharmacology and Therapeutics, Roswell Park Cancer Institute, Buffalo, New York, 14263

^cOrekhovich Institute of Biomedical Chemistry, Moscow 119121, Russia

^dDepartment of Pathology, Roswell Park Cancer Institute, Buffalo, New York, 14263

^eDepartment of Pharmacology, University of Michigan, Ann Arbor, Michigan, 48109

Abstract

Melanoma progression is associated with increased invasion and, often, decreased levels of microphthalmia-associated transcription factor (MITF). Accordingly, downregulation of MITF induces invasion in melanoma cells, however little is known about the underlying mechanisms. Here, we report for the first time that depletion of MITF results in elevation of intracellular GTP levels and increased amounts of active (GTP-bound) RAC1, RHO-A and RHO-C. Concomitantly, MITF-depleted cells display larger number of invadopodia and increased invasion. We further demonstrate that the gene for guanosine monophosphate reductase (*GMPR*) is a direct MITF target, and that the partial repression of *GMPR* accounts mostly for the above phenotypes in MITF-depleted cells. Reciprocally, transactivation of *GMPR* is required for MITF-dependent suppression of melanoma cell invasion, tumorigenicity, and lung colonization. Moreover, loss of *GMPR* accompanies downregulation of MITF in vemurafenib-resistant BRAF^{V600E}-melanoma

Users may view, print, copy, and download text and data-mine the content in such documents, for the purposes of academic research, subject always to the full Conditions of use:http://www.nature.com/authors/editorial_policies/license.html#terms

*Corresponding author: Mikhail A. Nikiforov, Department of Cell Stress Biology, Roswell Park Cancer Institute, BLSC L3-317, Buffalo, New York, 14263, Phone: (716) 845-3374, Fax: (716) 845-3944, mikhail.nikiforov@roswellpark.org.

#These authors contributed equally to the work

\$Current address: Department of Pathology and Moores Cancer Center, University of California, San Diego, La Jolla, California, 92093

Competing financial interests

The authors declare no competing financial interests.

Author contributions

A.B-S., A.B., and M.A.N. designed the experiments and wrote the manuscript; A.B-S. and A.B. performed most of the experiments and analyzed the data; S.M., E.E.F., J.A.W., E.K.M., P.J., M.K., C.E.F., A.E.B., N.I.K., B.C.L., L.M.R., S.B., and J.A. performed some of the experiments; W.B. performed and scored the IHC staining; D.S.S. supervised part of the study; M.A.N. conceived the initial hypothesis and supervised the study. A.B-S. and A.B. contributed equally to this study. All authors discussed the results and commented on the manuscript.

cells and underlies the increased invasion in these cells. Our data uncover novel mechanisms linking MITF-dependent inhibition of invasion to suppression of guanylate metabolism.

Keywords

microphthalmia-associated transcription factor (MITF); invasion; GTP; guanosine monophosphate reductase (GMPR); vemurafenib-resistance

INTRODUCTION

Metastatic melanoma is one of the most aggressive forms of human cancers (1) and the only malignancy with a steadily increasing incidence over the past 50 years (2). Acquisition of invasion is an important prerequisite of metastasis and is considered a critical event associated with poor prognosis in melanoma patients (3). Tumor cell invasion is a complex process that, among other steps, involves formation of invadopodia, which are subcellular actin-rich structures that recruit proteases and protrude into the extracellular matrix (ECM) (4). In melanoma cells, the ability to form invadopodia and invade through the ECM largely depends on the activity of several members of the RHO-GTPase family of small (~21kDa) guanine nucleotide binding proteins (G-proteins) (5), of which RAC1 plays the most prominent role (6). Consistently, an activating RAC1^{P29S} mutation was identified as the 3rd most frequent in a cohort of sun-exposed melanomas (7).

Our recent studies have established that in tumor cells, including melanoma, invasion is regulated by several enzymes involved in the guanylate metabolism pathway (8, 9). This regulation occurs through modulation of intracellular GTP pools, which affects the activity of several members of RHO-GTPase family (9–11). Furthermore, the importance of GTP biosynthesis enzymes in regulation of tumor cell invasion has been recently confirmed in a separate study (12). Notably, the mRNA levels of the gene encoding one of the guanylate metabolism enzymes, guanosine monophosphate reductase (GMPR), are downregulated in metastatic melanoma cell lines and metastatic melanoma patients in comparison to normal human melanocytes and primary tumors, respectively (9). However, transcription factor(s) regulating *GMPR* expression are unknown.

Melanoma progression, like many other cancers, is accompanied by loss of differentiation programs and increase in cell plasticity including invasion, which also correlates with decreased levels of microphthalmia-associated transcription factor (MITF) (13, 14). MITF belongs to the basic helix-loop-helix (bHLH)-Zip protein family and is composed of at least ten isoforms (15, 16). Expression of the M-isoform is restricted to cells of melanocytic lineage where it plays a critical role in terminal differentiation (15, 16)

MITF has been characterized as both a melanoma oncogene (17, 18) and an invasion suppressor (13, 19–22); these seemingly contradictory reports on the role of MITF in melanoma progression have been reconciled with the proposal of a “rheostat model”. In this model, high levels of MITF inhibit proliferation and induce terminal differentiation, moderate levels correspond to rapidly proliferating cells but with limited invasive potential, and low levels of MITF correspond to slowly proliferating but highly invasive cells (20, 23).

Accordingly, MITF has been shown to suppress melanoma cell invasion in cultured cells (20, 22) and the growth of melanoma xenografts in immunocompromised mice (13), which may occur due to impaired invasion (24). Intriguingly, several recent papers revealed that during *in vitro* or *in vivo* selection for resistance to the BRAF^{V600E} inhibitor vemurafenib, which is widely used in clinical settings (25, 26), melanoma cells often down-regulate MITF expression and acquire increased invasion (27–31). Yet, the molecular mechanisms underlying invasion-suppressing functions of MITF in naïve and vemurafenib-resistant cells are not well-understood (23).

In answer to these questions, in the current manuscript we investigated the role of *GMPR* transcriptional regulation and *GMPR* downstream processes in the MITF-dependent control of melanoma cell invasion.

RESULTS

MITF directly regulates *GMPR* expression

GMPR mRNA and protein levels are downregulated in melanoma cells and patient samples (9); however, *GMPR* transcriptional regulators are unknown. Based on the available information about transcription factors controlling melanoma cell invasion, we hypothesized that *GMPR* expression is regulated by MITF. To test this hypothesis, we utilized SK-Mel-28 and 501Mel metastatic melanoma cells since MITF-dependent suppression of invasion has been previously reported in these cells (20, 22, 32). In both cell lines, shRNA-mediated depletion of MITF downregulated *GMPR* mRNA and protein levels as was evidenced by Q-RT-PCR and immunoblotting, respectively (Fig. 1A). In a reciprocal experiment, ectopic expression of MITF cDNA in SK-Mel-28 and primary tumor-derived A375 cells led to an increase in *GMPR* at mRNA and protein levels (Fig. 1B. 501Mel cells could not be used due to the already high endogenous levels of MITF). A similar MITF-dependent pattern of *GMPR* expression was detected in normal human melanocytes (NHM) (Supplementary Fig. S1).

Analysis of the *GMPR* regulatory regions 10Kb upstream and 1 Kb downstream of the transcription start site identified several putative MITF binding sites consisting of E-boxes (CAYRTG) and M-boxes (TCAYRTG or CAYRTGA) (32) (Fig. 1C). Alignment of human and mouse *GMPR* promoters revealed substantial homology in the region most proximal to the TSS, containing three closely spaced MITF potential binding sites one of which (box #7) was perfectly conserved (Supplementary Fig S2A)..

To test for MITF direct binding to the *GMPR* proximal regulatory region, we performed chromatin immunoprecipitation (ChIP) assay in SK-Mel-28 cells ectopically expressing MITF using a commercially available MITF antibody or IgG as control (see Material and Methods). Following ChIP, the precipitated DNA was probed in Q-PCR with primers specific to the proximal region (Fig. 1C). In parallel, the precipitated DNA was probed with primers to a distal, non-conserved, putative binding site (box 4). Following normalization of PCR signals, a significant enrichment (15.8 fold) was detected with the primers corresponding to the proximal region in the DNA precipitated with MITF-specific versus

IgG antibodies (Fig. 1D), while no enrichment was detected using primers to either the *GMPR* distal promoter region.

These findings were further validated in more physiological settings by performing ChIP in wild type SK-Mel-28 cells expressing only endogenous levels of MITF. A lower, but still statistically significant enrichment was identified of the proximal but not distal regions of the *GMPR* promoter (Fig. 1D).

To further assess the importance of these E/M boxes for MITF binding to the *GMPR* promoter, we cloned the ~250bp proximal regulatory region of the *GMPR* promoter into the pGL3 promoter luciferase reporter system. Additionally, we mutated the putative MITF binding region to assess its functionality (see Supplementary Fig. S2B). HEK293T cells were transiently transfected with either the empty vector (pGL3) or the vector containing the wild-type sequence or the mutant for the *GMPR* promoter region of interest, in combination with no or increasing amounts of the MITF expression vector and with pRLSV40 plasmid expressing the Renilla luciferase gene. 48 hours later, firefly luciferase and Renilla signals were detected via Dual-Luciferase Assay Kit (Promega) and firefly luciferase signals were normalized by corresponding Renilla signals. As shown in Fig. 1E, the WT-*GMPR* construct displayed increasing amounts of luciferase activity proportionally to the amounts of MITF supplied, indicating that MITF does indeed bind to this region in the *GMPR* promoter. Mutation of the putative binding site abrogated such response (Fig. 1E).

To evaluate whether *GMPR* expression correlates with MITF levels in human specimens, we performed MITF immunohistochemistry (IHC) staining of primary and distant-organ metastatic melanoma specimens, using the same tissue sections that we had previously used to assess *GMPR* expression levels (9). We found that MITF expression was significantly decreased during melanoma progression (Fig. 2A) in agreement with previous reports (20, 33) and similarly to our previous findings of *GMPR* expression pattern (9). To further examine the pattern of expression of MITF and *GMPR* within the same specimens, we classified their IHC indices of 3 and below as “low” and 4 and above as “high”. A proportion test was used to determine if there was significant concordance between MITF and *GMPR* expression among the primary thin and thick, and the metastatic samples. We found a significant concordance in all three disease stages (thin $p=0.033$, thick $p=0.035$, metastatic $p=2.211e-05$; Fig. 2B and Supplementary Fig. 3).

Taken together, our data demonstrate that *GMPR* is a *bona fide* MITF target gene in cultured melanocytic cells and human melanoma specimens.

MITF depletion increases melanoma cell invasion and intracellular GTP pools

In order to investigate the mechanisms underlying increased invasion in response to MITF downregulation, we first sought to recapitulate this phenotype in cells where it has been originally reported (SK-Mel-28, 501Mel). To this end, the MITF-depleted melanoma cells described in Fig. 1a were tested for invasion through Matrigel™ in a Boyden chamber assay. In agreement with previous studies (20, 22), we detected a ~3–6 fold increase in invasion of MITF-depleted cells over control cells (Fig. 3A,B) concomitant with a slight decrease in

proliferation rate (also in agreement with published data (18)) as determined by cell counting (data not shown).

To establish the role of guanylate metabolism in MITF invasion-suppressing activity, we quantified GTP levels in SK-Mel-28 and 501Mel cells depleted of MITF. Depletion of MITF led to a modest (6%-9%) but reproducible and statistically significant increase in GTP levels (Fig. 3C). Similar increase was detected in SK-Mel-28 cells depleted of GMPR approximately to the same levels as those achieved via MITF depletion (Supplementary Fig. S4), or detected previously in GMPR-depleted NHM (9). Importantly, overexpression of GMPR in MITF-depleted cells reduced the GTP levels to those in control cells (Fig. 3D,E).

MITF depletion increases RHO GTPases activity and extra-cellular matrix degradation

GMPR downregulates invasion of melanoma cells by decreasing the intracellular amounts of GTP and inhibiting the activity of several small GTPases, among which, RAC1 is the most affected (9). RAC1 has been also shown to play an important role in melanoma cells invasion (9, 34). Based on these observations, we hypothesized that inhibition of RAC1 activity plays a major role in MITF-dependent suppression of invasion.

To test this hypothesis, we assessed RAC1 activity through a GTP pull-down assay (9) in control and MITF-depleted SK-Mel-28 and 501Mel cells. MITF depletion resulted in a ~3 fold increase in the amounts of GTP-bound (active) RAC1 in MITF-depleted versus control cells (Fig. 4A). We have previously shown that GMPR manipulations could also affect the activation status of RHO-A and RHO-C, although to a lesser extent than RAC1 (9). Consistently, MITF depletion increased the proportion of active RHO-A and RHO-C as well (Fig. 4B).

It has been previously shown that RHO-A-activated kinase (ROCK) inhibition can blunt the increased invasiveness of MITF-depleted cells (20). To test whether RAC1 activation is important for the increased invasion of MITF-depleted SK-Mel-28 cells, we utilized a well-characterized inhibitor of RAC1 NSC23766. Through titration, we identified a concentration of 25 μ M at which NSC23766 did not affect invasion in control cells, but decreased invasion in MITF-depleted cells (Fig. 4C), suggesting the leading role of RAC1 activation in increased invasion of these cells.

The activity of RAC1 has been linked to the ability of melanoma cells to form invadopodia and degrade ECM (34, 35). Therefore, we tested control and MITF-depleted SK-Mel-28 cells in the gelatin degradation assay. At the same time, cells were stained with phalloidin to visualize active invadopodia (actin puncta matching with areas of gelatin degradation) as previously described (9). MITF depletion resulted in a greater number of cells with degradation and increased number of active invadopodia per cell compared to control cells (Supplementary Fig. S5A).

In summary, our data demonstrate that downregulation of MITF induces melanoma cell invasion in large part via inhibition of GMPR-dependent suppression of RAC1 activity, formation of invadopodia and matrix degradation.

GMPR downregulation underlies increased invasion in vemurafenib-resistant cells

Several reports have demonstrated that melanoma cells selected for resistance to BRAF^{V600E} inhibitors, including the clinically utilized small molecule vemurafenib, acquire increased invasion compared to parental counterparts (27, 36, 37). This increase in invasion has been attributed to the loss of MITF (27–29). Therefore, we hypothesized that the invasive phenotype of vemurafenib-resistant melanoma cells depends on downregulation of GMPR. To test this hypothesis, we first determined whether inhibition of BRAF^{V600E} signaling by vemurafenib affects the levels of GMPR as it has been shown for MITF (27). Indeed, treatment of SK-Mel-28, Colo-679, and WM793 human melanoma cells with vemurafenib (PLX4032) induces MITF and GMPR levels (Fig. 5A).

Next, we selected SK-Mel-28, Colo-679, and A375 cells for resistance to 10 μ M vemurafenib for over 6 months as previously described (27) (see Materials and Methods and Supplementary Fig. S6). In line with this report (27), we observed either maintenance (A375) or loss (SK-Mel-28, Colo-679) of MITF endogenous levels in resistant cells when compared to parental cells (Fig. 5B). Notably, cells with decreased MITF levels also displayed concomitant loss of GMPR and increased invasion (Fig. 5B,C), whereas A375 cells, which displayed no changes in MITF levels, retained GMPR (Fig. 5B) and did not display any changes in invasion (Fig. 5C).

To investigate whether the loss of GMPR was responsible for the increased invasion in resistant cells, we restored GMPR levels in SK-Mel-28R and Colo-679R approximately to the levels detected in parental cell lines (Fig. 5B) followed by an invasion assay (Fig. 5C). Restoration of GMPR levels did not affect MITF levels but did decrease invasion in vemurafenib resistant cells, close to the levels detected in parental cells (Fig. 5B,C). Collectively, our data strongly suggest that increased invasion in vemurafenib-resistant cells depends on suppression of the MITF-GMPR axis.

Ectopic expression of MITF suppresses RHO-GTPase activation and invadopodia formation

Data presented above argue that MITF depletion leads to increase in invasion due to downregulation of GMPR. On the other hand, MITF overexpression has been shown to suppress invasion and tumorigenicity in melanoma cells (20, 22, 38). Therefore, we were intrigued by the possibility that this phenomenon could be explained as well through MITF-mediated regulation of GMPR (Fig.1) and GMPR-dependent pathways.

Ectopic expression of MITF in SK-Mel-28 and A375 cells led to upregulation of GMPR and a ~50% decrease in invasion compared to the cells carrying empty-vector control, which was reverted by guanosine supplementation (Fig 6A). Nucleotide quantification by HPLC showed that MITF over-expression reduced GTP by 19% and 9% (in SK-Mel-28 and A375, respectively), whereas supplementation with guanosine fully abrogated this effect.

Moreover, overexpression of MITF suppressed activation of RAC1, RHO-A, and RHO-C, as determined by GTPase pull-down assay (Fig. 6C,D). Finally, gelatin degradation and invadopodia formation were decreased in cells overexpressing MITF (Supplementary Fig. S5B).

GMPR is critical for MITF-dependent suppression of melanoma cell invasion, tumorigenicity, and lung colonization

To further test whether MITF suppression of invasion depends on its ability to upregulate GMPR, we infected human SK-Mel-28 and A375, and murine B16-F10 melanoma cells with control or GMPR shRNAs (9), followed by super-infection with MITF cDNA or empty-vector (pLVp) (Fig. 7A). Of note, the shRNAs designed toward human GMPR inhibited also the mouse Gmpr. In cells from all cell lines, MITF overexpression suppressed invasion of melanoma cells by ~2 fold (Fig. 7B), while partial depletion of GMPR, carried out to compensate for GMPR induction by MITF, efficiently blunted the ability of MITF to reduce invasion (Fig. 7B). We were unable to manipulate the GMPR shRNAs viral titers in such ways as to achieve reduction of GMPR levels exactly to the ones detected in control cells. As a result, we obtained a slightly stronger GMPR repression (Fig. 7A), which led to a more pronounced invasion in these cells compared to control cells.

We have previously demonstrated that the invasion of GMPR-depleted SK-Mel-28 melanoma cells plays a critical role in their ability to efficiently form xenograft tumors in immunocompromised mice (9). In the same paper, we demonstrated that GMPR suppresses invasion of melanoma xenografts at the tumor margin in such mice. Previously, invasion as a mean of release of spatial constraints has been demonstrated to increase xenograft volume (24). To test whether suppression of xenograft growth by MITF depends on its ability to upregulate *GMPR*, we inoculated subcutaneously in both flanks of *scid/scid* (SCID) mice the SK-Mel-28 and A375 cell populations overexpressing MITF and depleted of GMPR as described above. Once tumors became palpable, their size was recorded every 5 days (SK-Mel-28) or 2 days (A375). In both cell lines, over-expression of MITF caused a significant retardation in tumor growth (Fig. 7C). Reduction of GMPR levels in melanoma cells overexpressing MITF (Fig. 7A) increased the growth of MITF-overexpressing xenografts (Fig. 7C), strongly suggesting a functional role of GMPR in MITF-dependent suppression of melanoma cell xenograft growth *in vivo*.

To assess the role of GMPR in MITF-dependent control of melanoma cell experimental metastasis B16-F10 cells described above were injected intravenously in syngeneic wild-type C57Bl/6 mice. Animals were sacrificed 12 days post-injection and the number of pulmonary nodules for each cohort was recorded. MITF-expressing melanoma cells demonstrated lower lung colonization potential than control cells, whereas depletion of GMPR in MITF-overexpressing cells fully compensated for such decrease (Fig 7D and Supplementary Fig 7) suggesting a pivotal role of GMPR in MITF-dependent suppression of melanoma cell tumorigenicity and experimental metastasis.

DISCUSSION

In the course of melanomagenesis, increase in invasion is often accompanied by suppression of differentiation programs (39). These phenotypes are oppositely controlled by the master regulator of melanocyte development microphthalmia-associated transcription factor (MITF) (14, 21), which appears to play a dualistic role in melanoma progression (18, 20, 40, 41). MITF has been reported to have oncogenic properties, and its amplification has been detected in ~15% of advanced human melanoma specimens carrying the common

BRAF^{V600E} mutation (40). Accordingly, MITF has been proposed to contribute to melanoma cell survival through upregulation of the anti-apoptotic gene *BCL2* (17). On the contrary other groups reported that BRAF^{V600E} suppresses MITF expression (18), and MITF has also been shown to suppress invasion in cells from several melanoma lines (20–23). Finally, published and our own data demonstrate that MITF expression decreases during melanoma progression (Fig. 2A and Ref (20, 33)).

Recently, to encompass these multiple and often contradictory reports on MITF activity, a “rheostat” model of MITF functioning has been proposed. According to this model, high MITF levels inhibit proliferation and induce differentiation of melanoma cells; moderate levels of MITF promote proliferation; low MITF levels cause slowly proliferation/high invasion phenotypes (14, 20).

The mechanisms underlying MITF invasion-suppressing activity have been addressed in detail only in a few studies. Thus, it has been shown that MITF interferes with production of MT1-MMP (19) or transcriptional activation of miR222/221 (42), a microRNA that is capable of invasion initiation in melanoma cells (43). Additionally, two papers reported different pathways through which MITF suppresses the activity of Rho-associated coiled-coil containing protein kinase 1 (ROCK1) (19, 20), an important regulator of tumor cell invasion (44) acting downstream of small GTPase RHO-A. Our recent report on the ability of GMPR to suppress activity of several RHO-GTPases, including RHO-A (9) in combination with the current data suggest that upregulation of GMPR could account at least in part for the effects described in the above studies. Interestingly, in the same study we discovered that the activity of RAC1 was affected by GMPR-dependent changes in GTP to the highest extent among members of RHO-GTPase family (9). Our findings are in agreement with previous reports establishing the pivotal role of RAC1 in melanoma progression, including a recent paper that identified an activating mutation in RAC1 (RAC1^{P29S}) as the 3rd most frequent in a cohort of sun-exposed melanomas (6, 7).

Due to the above reasons, in the current paper we focused on the possible connection between MITF and RAC1. We demonstrated that MITF suppresses activity of RAC1 and RAC1-dependent processes (Fig.4A and 6C) and that suppression of RAC1 activity blunts the increased invasiveness imparted by MITF depletion (Fig 4C). These data provide for the first time a functional link between these two major regulators of melanoma cell invasion. However, since MITF manipulations affect the activation of RHO-A and RHO-C as well (Fig.4B and 6D), it is possible that activities of other G-proteins (not limited to those of the RHO-GTPase family) as well as other MITF-dependent phenotypes are modulated by changes in intracellular GTP pools induced by MITF. These intriguing possibilities will be tested in future studies.

The important role of several *de novo* guanylate metabolism enzymes, including GMPR and its functional antagonists IMPDH2 and GMPS in regulation of RHO-GTPases activity and/or tumor cell invasion has been described by us and others (8–12, 45). The current paper demonstrates that transactivation of GMPR mediates the ability of MITF to suppress invasion, tumorigenicity and metastasis in melanoma cells, thus connecting this important transcription factor with regulation of guanylate metabolism (Fig. 7C,D). On the contrary,

regulation of GMPR does not account for all phenotypes induced by MITF. For instance, overexpression of MITF in melanoma cells suppresses invasion (Fig. 6A, Fig. 7B, and Ref(20, 22)) and slightly decreases proliferation rate (data not shown and Ref(20, 22, 32)), whereas ectopic expression of GMPR, while substantially affecting melanoma cell invasion, does not alter proliferation (9). Accordingly, GMPR suppresses tumorigenicity of several melanoma cell lines including SK-Mel-28 through inhibition of invasion (9); instead, MITF suppresses tumorigenicity in melanoma cells presumably by downregulating both invasion and proliferation (13, 20, 22, 32).

In light of these considerations, we were surprised to detect that both GMPR shRNAs in melanoma cells overexpressing MITF overcame MITF-induced suppression of tumor growth, and increased tumorigenicity in these cells to the levels of, or even above those in control cells (Fig. 7C). The observed effects are most likely due to the fact that shRNA-mediated depletion of GMPR overcompensated the increase in GMPR induced by MITF (Fig. 7A). As a result GMPR levels in these cells were lower than those in control cells (Fig. 7A), resulting in higher invasion (Fig. 7B) and subsequently higher tumorigenicity (Fig. 7C) compared to control cells, similarly to what we previously demonstrated with direct GMPR suppression (9). In Wawrzyniak et al we showed that the increased invasion of GMPR-depleted melanoma cells was crucial for their ability to efficiently form xenograft tumors in mice, while the same cells demonstrated no advantage in anchorage-independent growth in semi-solid agar (9). Moreover, in the same paper we demonstrated that GMPR suppressed invasion at tumor edge of melanoma xenografts in mice.

It is also conceivable that, in the course of tumor growth, cells overexpressing exogenous MITF adjusted its amounts to the levels promoting proliferation (see above for the description of the “rheostat model”). In this situation, tumors with higher invasion (due to GMPR levels lower than in control) and in addition expressing optimal levels of MITF may outgrow the control tumors. Similarly, B16-F10 cells ectopically expressing MITF fail to efficiently colonize the mouse lungs, and GMPR depletion is sufficient to fully revert the phenotype (Fig. 7D), directly supporting a major role of GMPR in MITF-dependent suppression of metastasis.

Data reported by us (9) and others (10–12) together with the current work strongly argue that even moderate changes in intracellular GTP pools have major phenotypic consequences. On the other hand, physiological variations in intracellular GTP pools have not been considered as a factor regulating RHO-GTPase activity because GTP levels in the cell were determined to be much higher than those required for saturation of these GTPases (0.5-2mM vs. 5–20µM) (46). However, currently measurements of GTP pools are always performed in total cell extracts which precludes detection of potential localized changes in GTP levels. In fact, it is plausible that GTP could be differentially distributed in various regions of the cell (as it has been already established for ATP (47, 48)), reaching concentrations comparable to the GTPase Kd for GTP. Unfortunately, the lack of instruments for monitoring intracellular GTP levels is the limiting factor to test this hypothesis.

Survival of melanoma patients bearing mutant BRAF^{V600E} allele has been significantly improved by the introduction of the small molecule inhibitor of BRAF^{V600E} vemurafenib

(25, 26); yet, only ~50% of patients demonstrate sufficient response to initial treatment, and almost all of them later develop progressive disease. It has been recently shown that acquisition of resistance to vemurafenib occurs, at least in part, through suppression of MITF (27–29). Accordingly, vemurafenib-resistant cells often possess a higher invasive potential compared to parental counterparts (27, 36, 37), a feature which may contribute to the enhanced growth of vemurafenib-resistant tumors. Our data argue that inhibition of MITF-GMPR axis plays a pivotal role in the increased invasion of vemurafenib resistant cells. In light of these findings, it would be crucial in the future to investigate whether GMPR levels are altered in melanoma specimens from patients who failed BRAF inhibitor therapy, and whether there is any correlation between GMPR levels and development of new metastases on therapy.

Importantly, we have recently revealed that inhibition of GMP synthase (GMPS, a functional antagonist of GMPR) by the fungus-derived antibiotic angustmycin A reduces the invasive capability of melanoma cells *in vitro* and tumorigenicity *in vivo* (8). It is therefore imaginable that suppression of melanoma cell invasion would enhance therapeutic potential of vemurafenib. Further investigations will be required to evaluate a combinatorial approach in which guanylate-suppressing agents are paired with existing therapy to improve treatment outcome and overcome drug resistance in melanoma.

MATERIALS AND METHODS

Cell Lines

Populations of normal human melanocytes were purchased from Invitrogen (Carlsbad, CA) and maintained in Medium 254 (Invitrogen) supplemented with Human Melanocyte Growth Supplement (Invitrogen). SK-Mel-28 human melanoma cell lines were obtained from Memorial Sloan Kettering Cancer Center. 501Mel human melanoma cell lines were a kind gift of Dr. Steven Rosenberg (Surgery Branch, National Cancer Institute, Bethesda, MD). Human A375 and Colo –679, and murine B16-F10 melanoma cell lines were obtained from ATCC. All cells were maintained in DMEM (except for Colo-679 cells which were maintained in RPMI) supplemented with 10% fetal calf serum, 2mM glutamine and penicillin-streptomycin antibiotics. Cells were kept at 37°C under an atmosphere of 5% carbon. To generate vemurafenib-resistant sublines (SK-Mel-28R, Colo-679R and A375R), parental cell lines were cultured in the presence of increasing concentrations of vemurafenib (from 1µM to 10µM) for over 6 months, followed by isolation and subsequent amplification of populations resistant to 10µM vemurafenib. During this time period, media and vemurafenib were replenished every 3 days. Resistant cells were maintained in media containing 10µM vemurafenib. Cell lines have been recently authenticated and verified for being mycoplasma-free using MycoAlert mycoplasma detection Kit purchased from Lonza (USA, Cat # LT07–318).

Antibodies and other reagents

The following antibodies were used: mouse monoclonal to MITF (clone D5, Cat# M3621, Dako, Carpinteria, CA); mouse monoclonal to GAPDH (Cat. # AM4300, Ambion, Austin, TX); rabbit polyclonal to GMPR (Cat # SAB1101144 Sigma-Aldrich, St. Louis,

MO); rabbit polyclonal to RAC1 (Cell Signaling, Cat# 2465); rabbit monoclonal to RHO-A (Cell Signaling, Cat# 2117); and rabbit monoclonal to RHO-C (Cell Signaling, Cat# 3430). The RAC1 inhibitor NSC23766 was purchased from Santa Cruz Biotechnology.

Immunoblotting

Whole cell extracts were prepared and analyzed as previously described (9). Where indicated, bands were quantified using ImageQuant software (GE Healthcare Life Sciences).

Immunohistochemistry

Formalin fixed and paraffin-embedded human melanocytic cells, cutaneous and metastatic melanoma tissues were processed at the Pathology Core Facility (Roswell Park Cancer Institute). Positive and negative control slides were supplied by the Pathology Core Facility and were included with every immunohistochemistry run. The MITF and GMPR antibodies were visualized with the Novocastra (Newcastle, UK) PowerVision kit, followed by Fast Red (Thermo Scientific). The slides were manually counterstained with hematoxylin. Human tissue specimens were scored for intensity of staining by a board-certified pathologist as described in Ref(9).

Plasmids and Infection

Lentiviral vectors encoding short-harpins RNA (shRNA) to MITF along with a non-silencing control vector were purchased from Sigma (shMITF #1 TRCN0000019119; shMITF #2 TRCN0000019123). shRNA constructs to GMPR were described previously (9). The MITF ORF was PCR-amplified from SK-Mel-28 cDNA with the following primers and cloned into the pLVp lentiviral expression system.

MITF_FWD (XbaI) ACACAtctaga**ATG**CTGGAAATGCTAGAATAT

MITF_REV (NheI) AGTCTgctagc**CTA**ACAAGTGTGCTCCGTCTC

The lentiviral infection protocol was described previously (49). All infected cells were briefly selected for resistance to puromycin and used in the described assays.

Matrigel™-based Invasion Assay

Invasion assay was performed using the BioCoat Matrigel™ invasion chambers (BD Bioscience, San Diego, CA) according to the manufacturer's instructions. Briefly, cells were seeded at 5×10^4 in 500 μ l of serum-free media into the upper compartment of the inserts; serum was added as a chemoattractant to the lower compartment. After 16hrs incubation, the non-invaded cells and the Matrigel™ were gently removed with a cotton swab; the invaded cells were stained, air-dried. Cells in 5 fields/insert were counted under the microscope. Experiments were performed in duplicates and repeated at least twice.

Combined Gelatin Degradation Assay

Coverslips were coated with warm Oregon Green® 488-conjugated gelatin (Invitrogen) as described in Ref(9). Melanoma cells (7.5×10^4) were seeded on the coverslips and after 16-hour incubation at 37°C they were fixed in 4% paraformaldehyde in PBS. After permeabilization in 0.05% triton x-100 in PBS, cells were stained with rhodamine-

conjugated phalloidin (Invitrogen, to visualize actin) and hoechst (Thermo Scientific, to visualize nuclei). Coverslips were mounted onto glass slides with aqua-mount media (Polysciences, Warrington, PA). Fluorescent images were captured using a Nikon TE2000-E inverted microscope equipped with Roper CoolSnap HQ CCD camera and MetaVue software.

Quantitative Real Time PCR

Total cellular RNA was isolated using the RNeasy Mini Kit (Qiagen, Valencia, CA). cDNA was prepared using cDNA reverse transcription kit (Invitrogen). Quantitative reverse transcription PCR was performed on 7900HT Fast Real-Time PCR System (Applied Biosystems, Carlsbad, CA) using Sybr GreenMaster Mix (Invitrogen) and the following primers:

Gene	Forward	Reverse
B2M	AGCGTACTCCAAAGATTCAGGTT	ATGATGCTGCTTACATGTCTCGAT
MITF	CTCACCATCAGCAACTCCTG	GATTGTCCTTTTTCTGCCTCTC
GMPR	GAGTGCCGTCATTGAGTGTG	TCCGTATGACCCGAAAACAT

PCR data were analyzed using sequence detection software 2.4 (Applied Biosystems).

Chromatin Immunoprecipitation (ChIP)

Interactions between MITF and the *GMPR* promoter were assessed as previously described in Ref(50). The following antibodies were used: mouse monoclonal to MITF (clone D5, Dako), and normal mouse IgG (Santa Cruz). The following primers were used for the analysis of MITF binding to the DNA: *GMPR* proximal promoter region (5'-CGAGGCTGCAGAAAAATGGAAG-3'), (5'-GTCCCATAGTAGTTGCTCAATGC-3'); *GMPR* distal promoter region (5'-AGCAATTCTTCTGCCTCAGC-3'), (5'-TGGCTAACACAGTGAAACCC -3')

Nucleotide Quantification

Cells were harvested by trypsinization, extracted with 0.4N perchloric acid and neutralized. NTPs were separated and quantified using a strong anion exchange column (Whatman, Hillshore, OR) with a gradient HPLC system (Waters Milford, MA) equipped with a photodiode array detector and controlled by Millennium 2010 software. Nucleotides were eluted with 0.005M ammonium phosphate, pH 2.8, for five minutes followed by a linear gradient to 0.75M ammonium phosphate, pH 3.7, over 60 minutes. Nucleotides were identified based on their UV absorbance spectrum and quantified at either 254 or 281 nm by comparison to the absorbance of a known amount of authentic standard.

GTP-bound GTPase Pull-Down Assay

The assay was performed using the GTPases Activation Assay kit (Cell Biolabs) according to the manufacturer's recommendations and as described previously (9). Samples were

resolved on polyacrylamide gels along with total lysates as control and visualized as described above.

Dual Luciferase Reporter Assay

The *GMPR* promoter region containing the E/M-boxes of interest was amplified with the following primers and cloned into the pGL3 promoter plasmid (Promega).

Fwd_KpnI- 5' ACACAGGTACCGAACTTCCTTTGGGGTATAGC 3'

Rev_SacI- 5' AGTCTGAGCTCGCATGGTAGTTACAGATTTGT 3'

Mutations at the desired site (see Supplementary Fig. S2B) were introduced with the Q5 site-directed mutagenesis kit (NEB) according to the manufacturer's instructions. The obtained constructs were mixed with pRLSV40 plasmid expressing the Renilla luciferase gene (Promega). HEK293T cells were transfected in triplicate with the plasmid mixtures, using SuperFect reagent (QIAGEN). At 48hrs after transfection, firefly luciferase and Renilla signals were detected via Dual-Luciferase Assay Kit (Promega). Firefly luciferase signals were normalized by corresponding Renilla signals.

Animal studies using a subcutaneous xenograft model

All experiments involving animals were approved by the institutional Animal Care and Use Committee. SK-Mel-28 and A375 cells (5.0×10^6 cells/flank, and 1.0×10^6 cells/flank, respectively).expressing control vector or MITF, superinfected with control vector or shRNA to GMPR were inoculated subcutaneously in both flanks of 4–6 week-old female SCID mice (Strain: C.B-Igh-1bIcrTac-Prkdcscid/Ros, bred and maintained by the in house transgenic mouse facility at RPCI) (n=5 per group) For all cohorts, the time of the appearance of tumor 2 mm in at least one dimension was recorded and tumors were measured thereafter every other day. Mice were sacrificed when tumor volume reached 2cm^3 or when a tumor became ulcerated. No animals were excluded from the study since all animals developed palpable tumors approximately 100mm^3 , 2–3 weeks post subcutaneous inoculation of cells. Animals were not randomized after the injections; however the animals were coded to “blind” the investigator until the experiment reached its endpoint.

In vivo experimental metastases model

All experiments involving animals were approved by the institutional Animal Care and Use Committee. 0.5×10^6 B16-F10 murine melanoma cells suspended in 100 μL sterile saline solution were injected intravenously into 6–8 week old male syngeneic wild-type C57Bl/6 mice (RPCI in house colony) (n=4 per group). Mice were killed 12 days later, and visible metastatic nodules on the lung surface were photographed and counted. No animals were excluded from the study since no animals developed signs of morbidity before the endpoint of the study. Animals were not randomized after the injections; however the animals were coded to “blind” the investigator until the experiment reached its endpoint.

Viability assay

Indicated human melanoma cells were seeded at 3,000 cell/well in a 96-well plate. Cells were treated for 48hrs with the indicated amounts of Vemurafenib (PLX4032, LC Labs) or vehicle control. Cell viability was assessed trypan blue exclusion cell counting.

Statistical Analysis

For animal studies, sample size was determined as a function of effect size ((difference in means)/(standard deviation)=2.0) for a two-sample t-test comparison assuming a significance level of 5%, a power of 90%, and a two-sided t-test. Each experiment was reproduced at least two times with consistent results. A two-tailed p value <0.05 was considered statistically significant for all analyses. Data was analyzed using parametric statistical methods such as t-test and proportion test for one or two group comparisons or ANOVA for several groups. Normal distribution was confirmed using normal probability plot (GraphPad Prism 6.0), variance was also assessed using GraphPad Prism 6.0 both within and between groups and were approximately the same.

Supplementary Material

Refer to Web version on PubMed Central for supplementary material.

Acknowledgments

We are grateful to Dr. Dominic Smiraglia (Roswell Park Cancer Institute) for critical reading of the manuscript and to the Pathology Resource Network and the Clinical Data Network at Roswell Park Cancer Institute for providing human specimens. This work has been supported by NIH grants CA120244 and CA190533 (M.A.N.), CA083081 (D.S.S.), Ruth L. Kirschstein National Research Service Award F32CA189622 (A.B-S.); American Cancer Society grant RSG-10-121-01 (M.A.N.); and Jennifer Linscott Tietgen Foundation (M.A.N.). This work was also supported in part by NCI Cancer Center Support Grant CA016056 to the Roswell Park Cancer Institute.

REFERENCES

1. Miller AJ, Mihm MC Jr. Melanoma. The New England journal of medicine. 2006; 355(1):51–65. [PubMed: 16822996]
2. Siegel RL, Miller KD, Jemal A. Cancer statistics, 2015. CA: a cancer journal for clinicians. 2015; 65(1):5–29. [PubMed: 25559415]
3. Curtin JA, Fridlyand J, Kageshita T, Patel HN, Busam KJ, Kutzner H, et al. Distinct sets of genetic alterations in melanoma. The New England journal of medicine. 2005; 353(20):2135–2147. [PubMed: 16291983]
4. Weaver AM. Invadopodia: specialized cell structures for cancer invasion. Clin Exp Metastasis. 2006; 23(2):97–105. [PubMed: 16830222]
5. Jaffe AB, Hall A. Rho GTPases: biochemistry and biology. Annu Rev Cell Dev Biol. 2005; 21:247–269. [PubMed: 16212495]
6. Halaban R. RAC1 and melanoma. Clin Ther. 2015; 37(3):682–685. [PubMed: 25465943]
7. Krauthammer M, Kong Y, Ha BH, Evans P, Bacchicchi A, McCusker JP, et al. Exome sequencing identifies recurrent somatic RAC1 mutations in melanoma. Nature genetics. 2012; 44(9):1006–1014. [PubMed: 22842228]
8. Bianchi-Smiraglia A, Wawrzyniak JA, Bagati A, Marvin EK, Ackroyd J, Moparthy S, et al. Pharmacological targeting of guanosine monophosphate synthase suppresses melanoma cell invasion and tumorigenicity. Cell death and differentiation. 2015

9. Wawrzyniak JA, Bianchi-Smiraglia A, Bshara W, Mannava S, Ackroyd J, Bagatis A, et al. A purine nucleotide biosynthesis enzyme guanosine monophosphate reductase is a suppressor of melanoma invasion. *Cell Reports*. 2013; 5(2):493–507. [PubMed: 24139804]
10. Hallett MA, Dagher PC, Atkinson SJ. Rho GTPases show differential sensitivity to nucleotide triphosphate depletion in a model of ischemic cell injury. *American journal of physiology Cell physiology*. 2003; 285(1):C129–C138. [PubMed: 12620811]
11. Mondin M, Moreau V, Genot E, Combe C, Ripoché J, Dubus I. Alterations in cytoskeletal protein expression by mycophenolic acid in human mesangial cells requires Rac inactivation. *Biochem Pharmacol*. 2007; 73(9):1491–1498. [PubMed: 17258688]
12. Kollareddy M, Dimitrova E, Vallabhaneni KC, Chan A, Le T, Chauhan KM, et al. Regulation of nucleotide metabolism by mutant p53 contributes to its gain-of-function activities. *Nat Commun*. 2015; 6:7389. [PubMed: 26067754]
13. Cheli Y, Giuliano S, Botton T, Rocchi S, Hofman V, Hofman P, et al. Mitf is the key molecular switch between mouse or human melanoma initiating cells and their differentiated progeny. *Oncogene*. 2011; 30(20):2307–2318. [PubMed: 21278797]
14. Hoek KS, Goding CR. Cancer stem cells versus phenotype-switching in melanoma. *Pigment cell & melanoma research*. 2010; 23(6):746–759. [PubMed: 20726948]
15. Cheli Y, Ohanna M, Ballotti R, Bertolotto C. Fifteen-year quest for microphthalmia-associated transcription factor target genes. *Pigment cell & melanoma research*. 2010; 23(1):27–40. [PubMed: 19995375]
16. Shibahara S, Takeda K, Yasumoto K, Udono T, Watanabe K, Saito H, et al. Microphthalmia-associated transcription factor (MITF): multiplicity in structure, function, and regulation. *The journal of investigative dermatology Symposium proceedings / the Society for Investigative Dermatology, Inc [and] European Society for Dermatological Research*. 2001; 6(1):99–104.
17. McGill GG, Horstmann M, Widlund HR, Du J, Motyckova G, Nishimura EK, et al. Bcl2 regulation by the melanocyte master regulator Mitf modulates lineage survival and melanoma cell viability. *Cell*. 2002; 109(6):707–718. [PubMed: 12086670]
18. Wellbrock C, Rana S, Paterson H, Pickersgill H, Brummelkamp T, Marais R. Oncogenic BRAF regulates melanoma proliferation through the lineage specific factor MITF. *PLoS one*. 2008; 3(7):e2734. [PubMed: 18628967]
19. Arozarena I, Bischof H, Gilby D, Belloni B, Dummer R, Wellbrock C. In melanoma, beta-catenin is a suppressor of invasion. *Oncogene*. 2011; 30(45):4531–4543. [PubMed: 21577209]
20. Carreira S, Goodall J, Denat L, Rodriguez M, Nuciforo P, Hoek KS, et al. Mitf regulation of Dial controls melanoma proliferation and invasiveness. *Genes & development*. 2006; 20(24):3426–3439. [PubMed: 17182868]
21. Cheli Y, Giuliano S, Fenouille N, Allegra M, Hofman V, Hofman P, et al. Hypoxia and MITF control metastatic behaviour in mouse and human melanoma cells. *Oncogene*. 2012; 31(19):2461–2470. [PubMed: 21996743]
22. Javelaud D, Alexaki VI, Pierrat MJ, Hoek KS, Dennler S, Van Kempen L, et al. GLI2 and M-MITF transcription factors control exclusive gene expression programs and inversely regulate invasion in human melanoma cells. *Pigment cell & melanoma research*. 2011; 24(5):932–943. [PubMed: 21801332]
23. Vachtenheim J, Ondrusova L. Microphthalmia-associated transcription factor expression levels in melanoma cells contribute to cell invasion and proliferation. *Experimental dermatology*. 2015; 24(7):481–484. [PubMed: 25866058]
24. Hotary KB, Allen ED, Brooks PC, Datta NS, Long MW, Weiss SJ. Membrane type I matrix metalloproteinase usurps tumor growth control imposed by the three-dimensional extracellular matrix. *Cell*. 2003; 114(1):33–45. [PubMed: 12859896]
25. Chapman PB, Hauschild A, Robert C, Haanen JB, Ascierto P, Larkin J, et al. Improved survival with vemurafenib in melanoma with BRAF V600E mutation. *The New England journal of medicine*. 2011; 364(26):2507–2516. [PubMed: 21639808]
26. Tsai J, Lee JT, Wang W, Zhang J, Cho H, Mamo S, et al. Discovery of a selective inhibitor of oncogenic B-Raf kinase with potent antimelanoma activity. *Proceedings of the National Academy of Sciences of the United States of America*. 2008; 105(8):3041–3046. [PubMed: 18287029]

27. Muller J, Krijgsman O, Tsoi J, Robert L, Hugo W, Song C, et al. Low MITF/AXL ratio predicts early resistance to multiple targeted drugs in melanoma. *Nat Commun.* 2014; 5:5712. [PubMed: 25502142]
28. Ji Z, Erin Chen Y, Kumar R, Taylor M, Jenny Njauw CN, Miao B, et al. MITF Modulates Therapeutic Resistance through EGFR Signaling. *J Invest Dermatol.* 2015; 135(7):1863–1872. [PubMed: 25789707]
29. Konieczkowski DJ, Johannessen CM, Abudayyeh O, Kim JW, Cooper ZA, Piris A, et al. A melanoma cell state distinction influences sensitivity to MAPK pathway inhibitors. *Cancer Discov.* 2014; 4(7):816–827. [PubMed: 24771846]
30. Paraiso KH, Das Thakur M, Fang B, Koomen JM, Fedorenko IV, John JK, et al. Ligand-independent EPHA2 signaling drives the adoption of a targeted therapy-mediated metastatic melanoma phenotype. *Cancer Discov.* 2015; 5(3):264–273. [PubMed: 25542447]
31. O'Connell MP, Marchbank K, Webster MR, Valiga AA, Kaur A, Vultur A, et al. Hypoxia induces phenotypic plasticity and therapy resistance in melanoma via the tyrosine kinase receptors ROR1 and ROR2. *Cancer Discov.* 2013; 3(12):1378–1393. [PubMed: 24104062]
32. Hoek KS, Schlegel NC, Eichhoff OM, Widmer DS, Praetorius C, Einarsson SO, et al. Novel MITF targets identified using a two-step DNA microarray strategy. *Pigment cell & melanoma research.* 2008; 21(6):665–676. [PubMed: 19067971]
33. Salti GI, Manougian T, Farolan M, Shilkaitis A, Majumdar D, Das Gupta TK. Microphthalmia transcription factor: a new prognostic marker in intermediate-thickness cutaneous malignant melanoma. *Cancer research.* 2000; 60(18):5012–5016. [PubMed: 11016620]
34. Bauer NN, Chen YW, Samant RS, Shevde LA, Fodstad O. Rac1 activity regulates proliferation of aggressive metastatic melanoma. *Exp Cell Res.* 2007; 313(18):3832–3839. [PubMed: 17904119]
35. Bartolome RA, Galvez BG, Longo N, Baleux F, Van Muijen GN, Sanchez-Mateos P, et al. Stromal cell-derived factor-1 α promotes melanoma cell invasion across basement membranes involving stimulation of membrane-type 1 matrix metalloproteinase and Rho GTPase activities. *Cancer research.* 2004; 64(7):2534–2543. [PubMed: 15059909]
36. Wang J, Huang SK, Marzese DM, Hsu SC, Kawas NP, Chong KK, et al. Epigenetic Changes of EGFR Have an Important Role in BRAF Inhibitor-Resistant Cutaneous Melanomas. *J Invest Dermatol.* 2015; 135(2):532–541. [PubMed: 25243790]
37. Zubrilov I, Sagi-Assif O, Izraely S, Meshel T, Ben-Menahem S, Ginat R, et al. Vemurafenib resistance selects for highly malignant brain and lung-metastasizing melanoma cells. *Cancer letters.* 2015; 361(1):86–96. [PubMed: 25725450]
38. Segura MF, Hanniford D, Menendez S, Reavie L, Zou X, Alvarez-Diaz S, et al. Aberrant miR-182 expression promotes melanoma metastasis by repressing FOXO3 and microphthalmia-associated transcription factor. *Proceedings of the National Academy of Sciences of the United States of America.* 2009; 106(6):1814–1819. [PubMed: 19188590]
39. Friedl P, Alexander S. Cancer invasion and the microenvironment: plasticity and reciprocity. *Cell.* 2011; 147(5):992–1009. [PubMed: 22118458]
40. Garraway LA, Widlund HR, Rubin MA, Getz G, Berger AJ, Ramaswamy S, et al. Integrative genomic analyses identify MITF as a lineage survival oncogene amplified in malignant melanoma. *Nature.* 2005; 436(7047):117–122. [PubMed: 16001072]
41. Wellbrock C, Marais R. Elevated expression of MITF counteracts B-RAF-stimulated melanocyte and melanoma cell proliferation. *The Journal of cell biology.* 2005; 170(5):703–708. [PubMed: 16129781]
42. Golan T, Messer AR, Amitai-Lange A, Melamed Z, Ohana R, Bell RE, et al. Interactions of Melanoma Cells with Distal Keratinocytes Trigger Metastasis via Notch Signaling Inhibition of MITF. *Mol Cell.* 2015
43. Felicetti F, Errico MC, Bottero L, Segnalini P, Stoppacciaro A, Biffoni M, et al. The promyelocytic leukemia zinc finger-microRNA-221/-222 pathway controls melanoma progression through multiple oncogenic mechanisms. *Cancer research.* 2008; 68(8):2745–2754. [PubMed: 18417445]
44. Kamai T, Tsujii T, Arai K, Takagi K, Asami H, Ito Y, et al. Significant association of Rho/ROCK pathway with invasion and metastasis of bladder cancer. *Clin Cancer Res.* 2003; 9(7):2632–2641. [PubMed: 12855641]

45. Arozarena I, Sanchez-Laorden B, Packer L, Hidalgo-Carcedo C, Hayward R, Viros A, et al. Oncogenic BRAF induces melanoma cell invasion by downregulating the cGMP-specific phosphodiesterase PDE5A. *Cancer cell*. 2011; 19(1):45–57. [PubMed: 21215707]
46. Franklin TJ, Twose PA. Reduction in beta-adrenergic response of cultured glioma cells following depletion of intracellular GTP. *Eur J Biochem*. 1977; 77(1):113–117. [PubMed: 198209]
47. Imamura H, Nhat KP, Togawa H, Saito K, Iino R, Kato-Yamada Y, et al. Visualization of ATP levels inside single living cells with fluorescence resonance energy transfer-based genetically encoded indicators. *Proceedings of the National Academy of Sciences of the United States of America*. 2009; 106(37):15651–15656. [PubMed: 19720993]
48. van Horsen R, Janssen E, Peters W, van de Pasch L, Lindert MM, van Dommelen MM, et al. Modulation of cell motility by spatial repositioning of enzymatic ATP/ADP exchange capacity. *The Journal of biological chemistry*. 2009; 284(3):1620–1627. [PubMed: 19008233]
49. Mannava S, Moparthy KC, Wheeler LJ, Natarajan V, Zucker SN, Fink EE, et al. Depletion of deoxyribonucleotide pools is an endogenous source of DNA damage in cells undergoing oncogene-induced senescence. *The American journal of pathology*. 2013; 182(1):142–151. [PubMed: 23245831]
50. Fink EE, Mannava S, Bagati A, Bianchi-Smiraglia A, Nair JR, Moparthy K, et al. Mitochondrial thioredoxin reductase regulates major cytotoxicity pathways of proteasome inhibitors in multiple myeloma cells. *Leukemia*. 2015

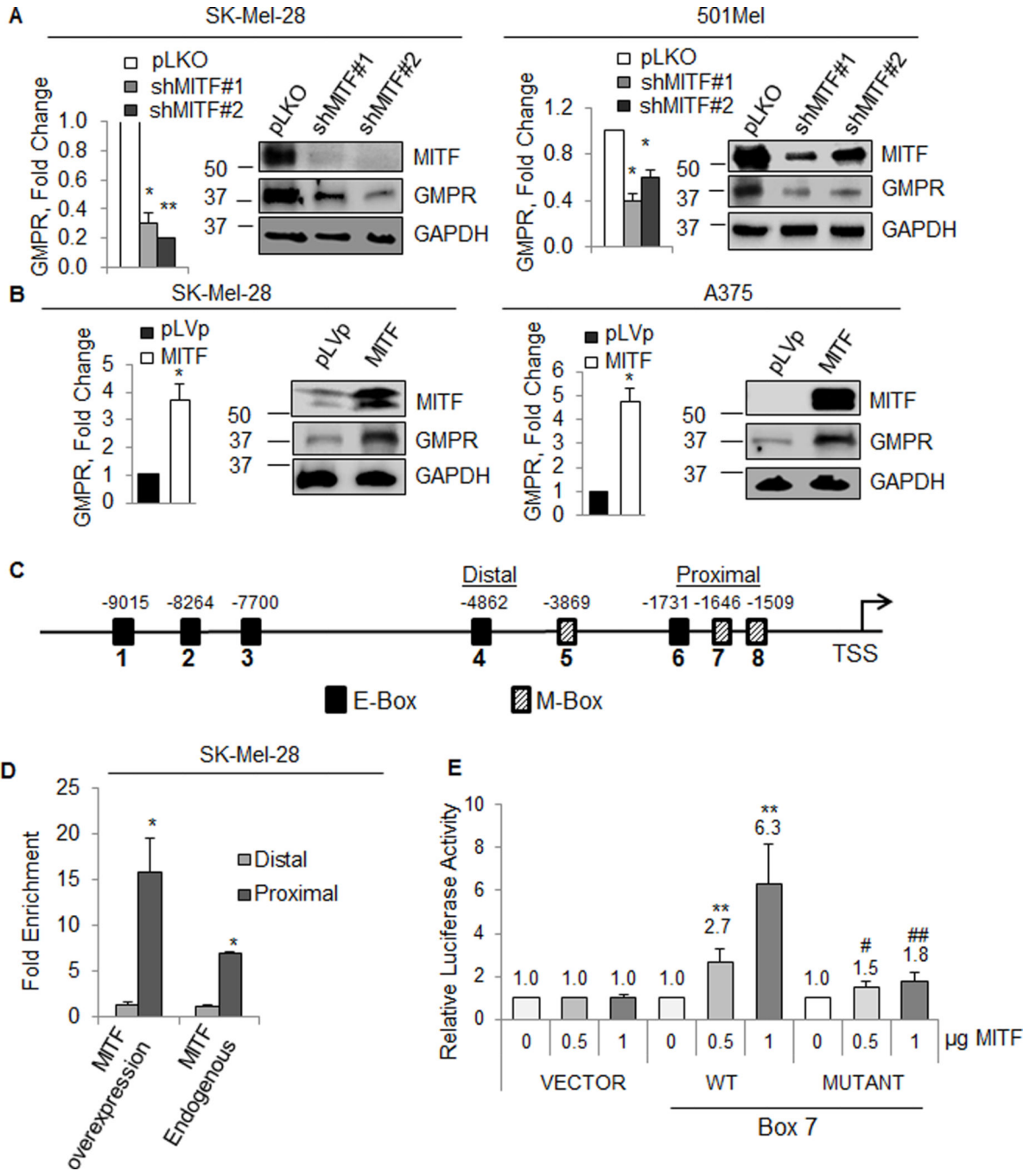


Figure 1. MITF controls GMPR expression

(A) SK-Mel-28 and 501Mel cells were transduced with an control shRNA (pLKO) or two different shRNAs to MITF (shMITF#1, #2) followed by reverse transcription quantitative PCR (RT-QPCR) (left panels) or immunoblotting the with indicated antibodies (right panels). (B) SK-Mel-28 and A375 cells were transduced with an empty vector (pLVp) or an overexpression vector encoding for MITF (MITF) followed by RT-QPCR analysis, (left panels) or immunoblotting with the indicated antibodies (right panels). The data represents

the average \pm SEM of at least two independent experiments performed in triplicates.

* $p < 0.05$, ** $p < 0.001$ by Student t-Test.

(C) Schematic of the human *GMPR* promoter up to 10Kb from the transcription starting site (TSS). Indicated are the E-box and M-box consensus sequences identified within, as well as the regions analyzed in chromatin immunoprecipitation (ChIP) analysis. (D) SK-Mel-28 cells overexpressing or not MITF were used for ChIP experiments with control (IgG) or a MITF-specific (MITF) antibodies. The resulting materials were probed by Q-PCR with primers specific for the most proximal region in the *GMPR* promoter (boxes 6–8) or a distal region (box4) as indicated in (C). All PCR signals were normalized by the corresponding PCR signals obtained in reactions with DNA precipitated with IgG antibodies. (E) The 250bp region containing the 3 most proximal putative MITF binding sites was cloned into the pGL3 promoter luciferase reporter system. Box 7 was mutated (see supplementary material) and the wild-type and mutant constructs were transduced into HEK293T cells along with the MITF expression vector and the pRLSV40 plasmid expressing the Renilla luciferase gene. Luciferase activity was measured 48hrs post-transfection. The data represents the average \pm SEM of at least 2 independent experiments performed in triplicates. * $p < 0.05$, ** $p < 0.001$ compared to control; # $p < 0.5$, ## $p < 0.001$ compared to GMPR at equivalent doses of MITF; statistic performed by Student t-Test.

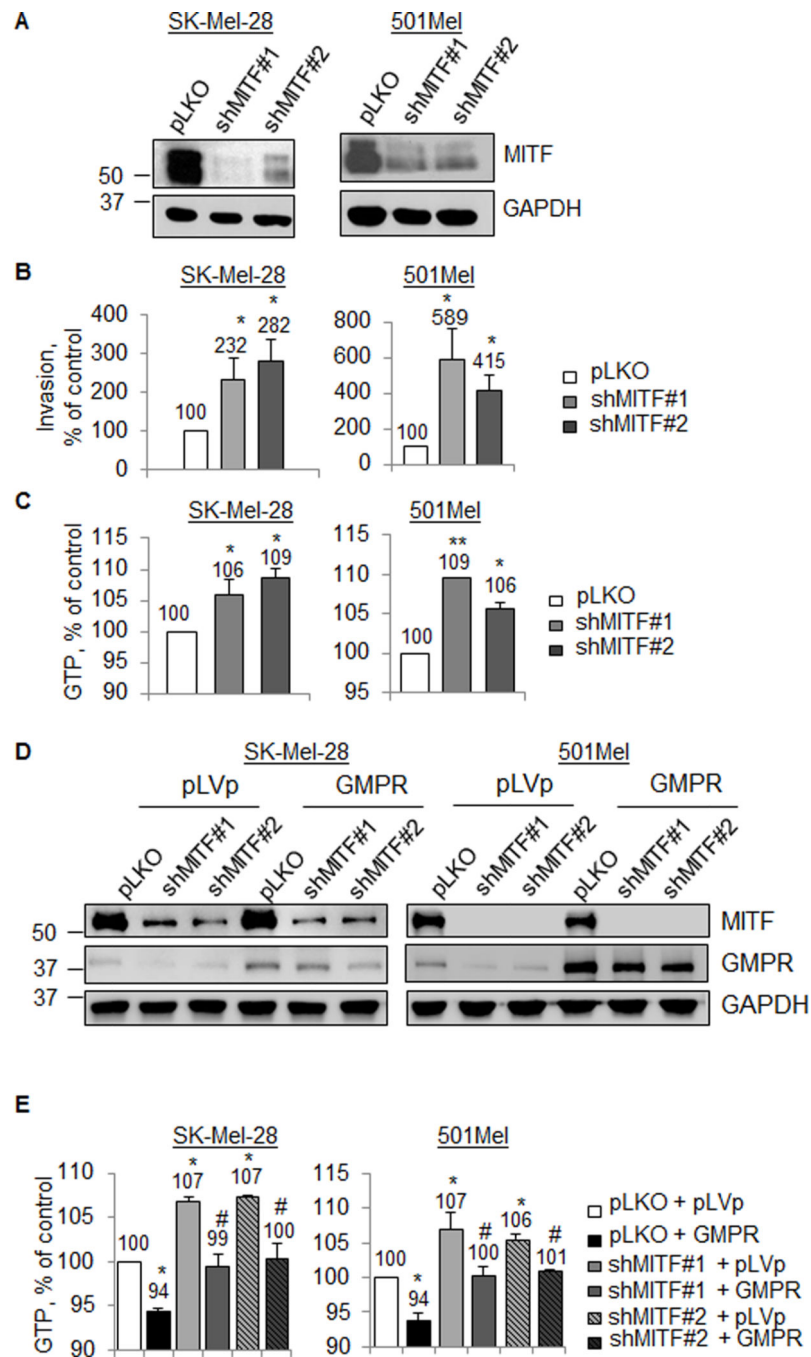


Figure 3. MITF controls melanoma cells invasion and GTP levels

SK-Mel-28 and 501Mel cells were transduced with control shRNA or two different shRNAs to MITF followed by (A) Immunoblotting with indicated antibodies and (B) invasion assay. (C) Nucleotides were extracted and quantified by HPLC as described in material and methods. (D) Cells as above were super-infected with an empty vector (pLVp) or an overexpression vector encoding for GMPR (GMPR). Shown are representative immunoblotting images of the manipulations. (E) Cells as in (D) were collected for nucleotide extraction and quantification as in (C). The data represents the average \pm SEM

of at least two independent experiments performed in duplicates. * $p < 0.05$, ** $p < 0.001$ compared to control; # $p < 0.05$ compared to shMITF + pLVp Statistics performed by Student t-Test.

Author Manuscript

Author Manuscript

Author Manuscript

Author Manuscript

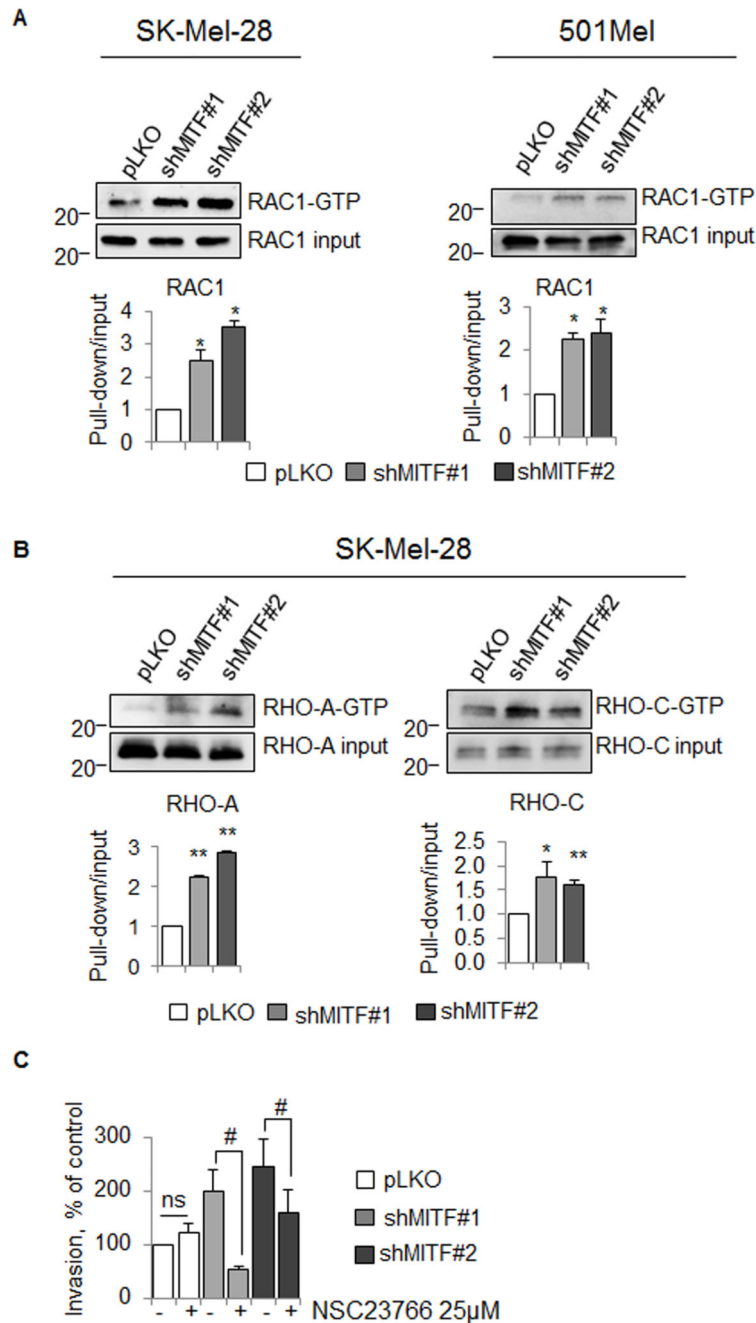


Figure 4. MITF depletion induces RHO-GTPases activation

(A) SK-Mel-28 and 501Mel cells transduced with control vector, or two different shRNAs to MITF were collected as described in Material and Methods and tested in the GTPase pull-down assay followed by immunoblotting with RAC1 antibodies (representative images and quantification of at least 2 independent experiments are shown). (B) SK-Mel-28 cells as in (A) were collected as described in Material and Methods and tested in the GTPase pull-down assay followed by immunoblotting with RHO-A and RHO-C antibodies (representative images and quantification of at least 2 independent experiments are shown).

(C) SK-Mel-28 cells as in (A) were treated with the RAC1 inhibitor NSC23766 (25 μ M) and tested for invasion through matrigel. The data represents the average \pm SEM of at least two independent. * p <0.05; ** p <0.01 compared to control; # p <0.05 compared to untreated. Statistics performed by Student t-Test.

Author Manuscript

Author Manuscript

Author Manuscript

Author Manuscript

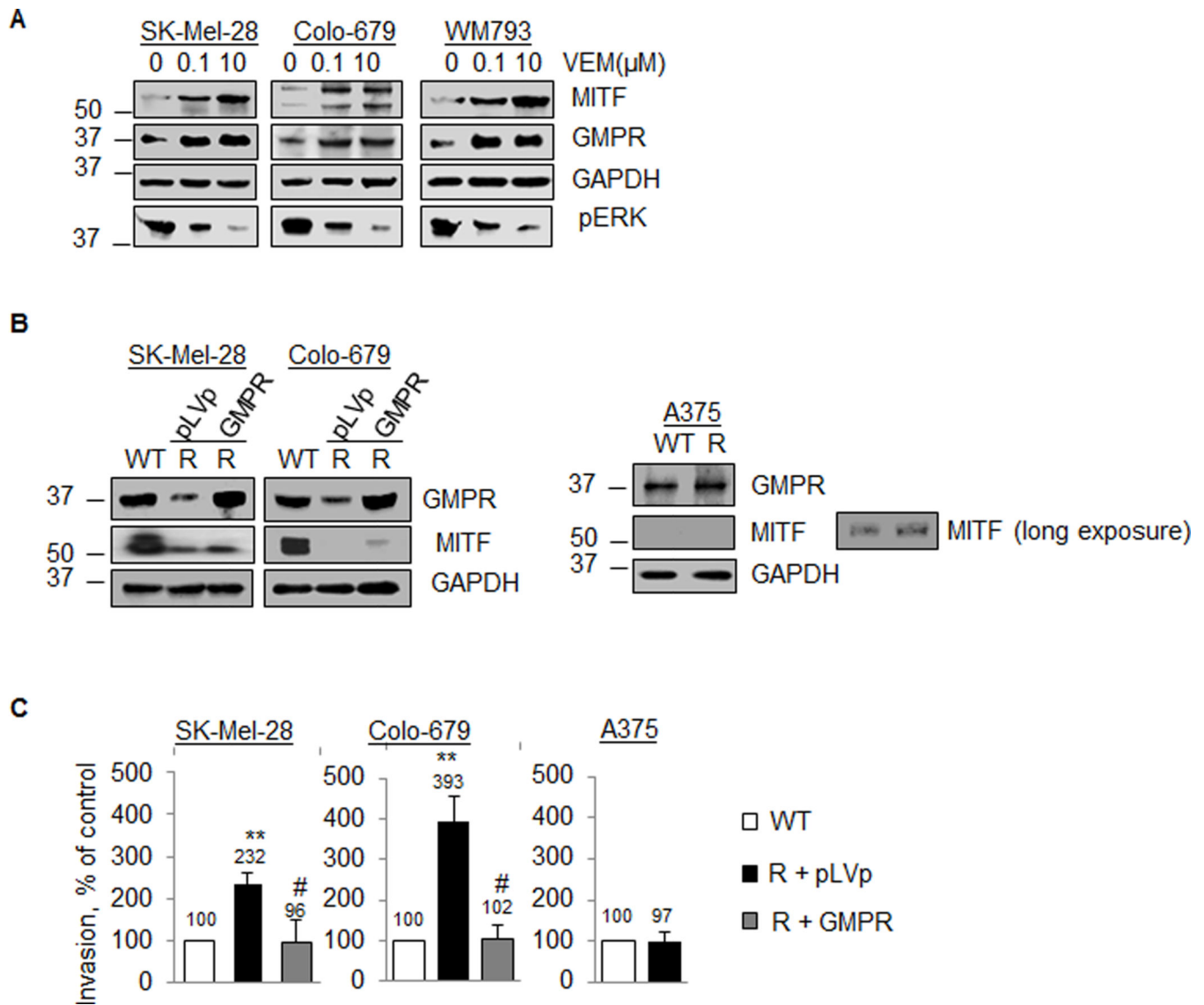


Figure 5. Increased invasion of vemurafenib-resistant cells depends on GMPR suppression

(A) SK-Mel-28, Colo-679, and WM793 human melanoma cells were treated with 0.1 or 10 μ M vemurafenib for 24hrs followed by immunoblotting with the indicated antibodies. (B) SK-Mel-28, Colo-679, and A375 human melanoma cells were selected for resistance to 10 μ M of vemurafenib (R, see material and methods). SK-Mel-28 and Colo-679 resistant cells were transduced with an empty vector (pLVp) or an overexpression vector encoding for GMPR (GMPR) followed by immunoblotting with the indicated antibodies. (C) Cells as in (B) were probed in invasion assay. * p <0.05; ** p <0.001 compared to WT; # p <0.05 compared to R+pLVp. Statistics performed by Student t-Test.

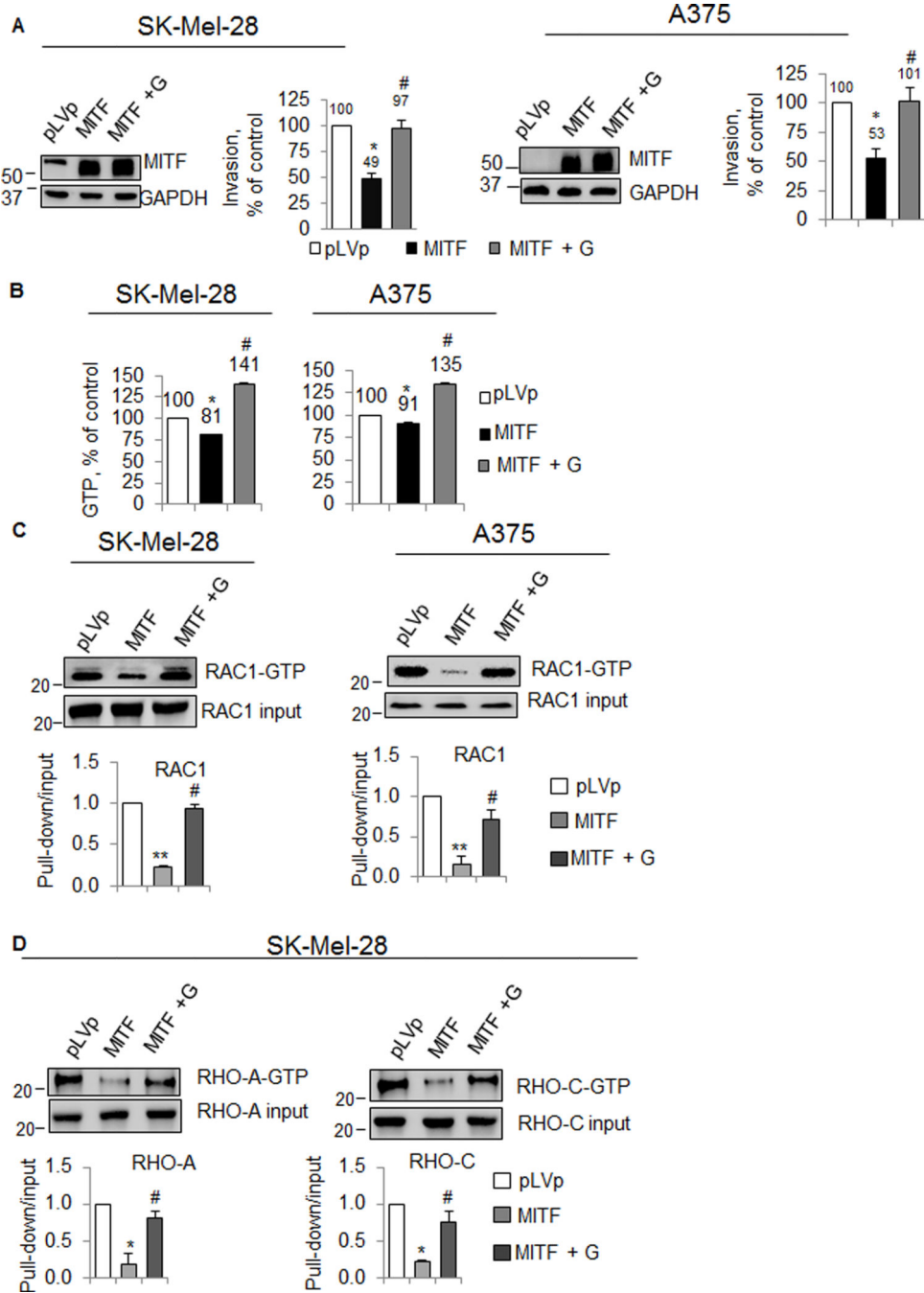


Figure 6. MITF overexpression suppresses RHO-GTPases activation and invasion
(A) SK-Mel-28 and A375 human melanoma cells were transduced with an empty vector or an overexpression vector encoding for MITF and probed in invasion assay; cells were supplemented or not with 100µM guanosine for 24hrs prior to and throughout the invasion assay. **(B)** Cells as in (A) were collected as described in Material and Methods and collected for nucleotides quantification by HPLC. **(C)** Cells as in (A) were collected as described in Material and Methods and tested in the GTPase pull-down assay followed by immunoblotting with RAC1 antibodies (representative images and quantification of at least

two independent experiments are shown). **(D)** SK-Mel-28 cells as in (A) were collected as described in Material and Methods and tested in the GTPase pull-down assay followed by immunoblotting with RHO-A and RHO-C antibodies (representative images and quantification of at least two independent experiments are shown). The data represents the average \pm SEM of at least two independent experiments performed in duplicates * $p < 0.05$; ** $p < 0.001$ compared to control; # $p < 0.05$ compared to MITF-overexpressing control. Statistics performed by Student t-Test.

Author Manuscript

Author Manuscript

Author Manuscript

Author Manuscript

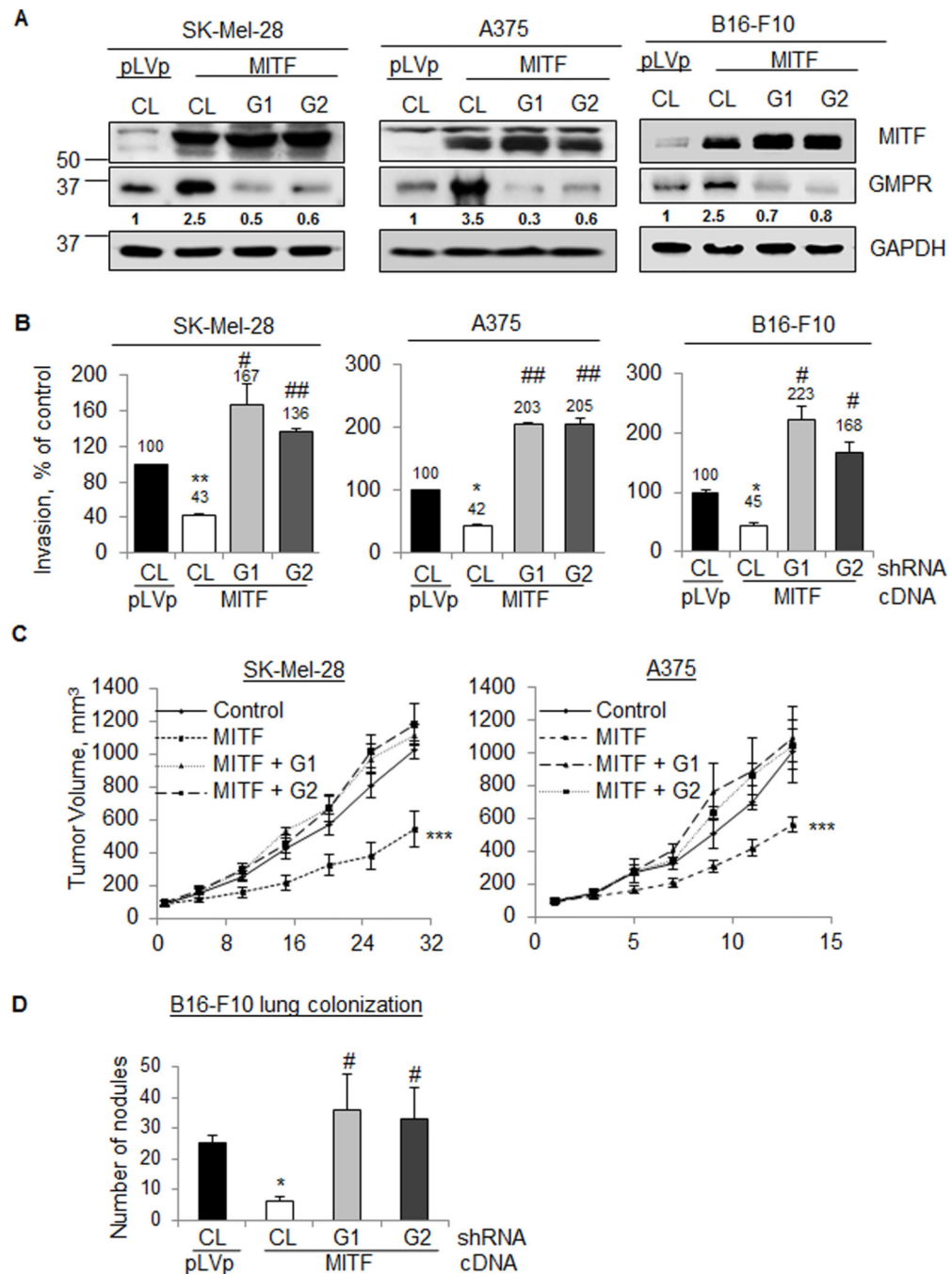


Figure 7. GMPR induction is critical for suppression of invasion and tumorigenicity by MITF (A) Human SK-Mel-28 and A375, and murine B16-F10 melanoma cells were transfected with an empty LVp or an overexpression vector encoding for MITF (MITF) and super-infected with an control shRNA (CL) or two different shRNAs to GMPR (G1 and G2). Of note, the shRNAs designed toward human GMPR inhibited also the mouse Gmpr. Cells were probed in immunoblotting with the indicated antibodies and the bands intensities were quantified using the ImageQuant software. The intensity of the GMPR band was divided by the intensity of the corresponding GAPDH band for each sample. The GMPR/GAPDH ratio

of pLVP+CL was then set as 1 and used to normalize accordingly all other ratios. **(B)** Cells as in (A) were probed in invasion assay. The data represents the average \pm SEM of at least two independent experiments performed in duplicates. * $p < 0.05$; ** $p < 0.001$ compared to control; # $p < 0.05$; ## $p < 0.001$ compared to MITF-overexpressing control. **(C)** SK-Mel-28 and A375 cells as in (A) were inoculated into both flanks of SCID mice (6 inoculation sites/sample). Tumor appearance was recorded when it reached at least 2 mm in one dimension and thereafter tumor xenografts were measured every other day. The data represents the average \pm SEM of the tumor size within each cohort. *** $p < 0.0001$ compared to controls. **(D)** B16-F10 cells as in (A) were injected intravenously into syngeneic wild-type C57Bl/6 mice, 4 mice per condition. Mice were sacrificed 12 days post-injection and the pulmonary nodules were counted. * $p < 0.05$ compared to control; # $p < 0.05$ compared to MITF-overexpressing control. Statistics performed by Student t-Test.